



中国科学院新疆天文台
XINJIANG ASTRONOMICAL OBSERVATORY, CAS

Reinvestigation of the electron fraction and electron Fermi energy of neutron star

Na Wang & Zhi-Fu Gao

Xinjiang Astronomical Observatory, CAS, China

12 May. 2017





Content

- **Introduction**
- **A general solution of electron
Fermi energy**
- **Numerical simulations**
- **Conclusions**



引言

- The electron fraction and the Fermi energy of relativistic electrons in circumstances of neutron stars (NSs) are two important physical parameters influencing directly weak-interaction processes including MURCA reactions, electron capture and so on
- This influence will change intrinsic equations of states , interior structure and heat evolution of a NS, and even affect whole properties of the star



Deduction

➤ Defining $E_F(e)$ for relativistic electrons: $E_F(e) \equiv [p_F^2(e)c^2 + m_e^2c^4]^{1/2}.(1)$

➤ Micro-state number in the weak-magnetic field approximation:

$$N_{pha} = \frac{g}{h^2} \int_0^{p_F(e)} 4\pi p^2 dp = \frac{8\pi}{3h^3} p_F^3(e).(2)$$

➤ Introducing dimensionless momentum

$$x_i = p_F(i) / m_i c \quad (i = e, n, p)$$

➤ According to Pauli's exclusion principle, electron number density is equal to its energy state density

$$n_e = N_{pha} = \frac{1}{3\pi^2 \lambda_e^3} x_e^3, \quad (3)$$

➤ By defining the mass of a baryon m_B

$$m_B \equiv \frac{1}{n} \sum_i n_i m_i = \frac{\sum_i n_i m_i}{\sum_i n_i A_i}, \quad (4),$$



➤ Matter density can be expressed as:

$$\rho = n_B m_B = \frac{n_e m_B}{Y_e}, \quad (5),$$

➤ Combining Eq.(4) and Eq.(5), we get:

$$x_e = \left(\frac{3\pi^2 \lambda_e^3}{m_u} \rho Y_e \right)^{1/3} \quad (6)$$

➤ Inserting $m_B = 1.66057 \times 10^{-24} \text{g}$ and

$\lambda_e = \frac{\hbar}{m_e c} = 3.8614 \times 10^{-11} \text{cm}$ into Eq.(6), we get:

$$x_e = 1.0088 \times 10^{-2} (Y_e \rho)^{1/3}, \quad (7)$$

➤ Utilizing $\mu_e = \frac{m_B}{m_u Y_e} = \frac{1}{Y_e}$, Eq.(5) is

$$\rho = \mu_e m_u n_e = 0.97395 \times 10^6 \mu_e x_e^3$$

rewritten as :

$$= 0.97395 \times 10^6 \frac{x_e^3}{Y_e} \text{g} \cdot \text{cm}^{-3} \quad (8)$$

➤ Combining Eq.(1) with Eqs. (7)

and (8), we get

$$E_F(e) = [1 + 1.018 \times 10^{-4} (\rho Y_e)^{2/3}]^{1/2} \times 0.511 \text{MeV}. \quad (9)$$



➤ From Shapiro & Teukolsky (1983), we get the electron fraction in the outer core region ($\rho \sim 0.5\rho_0 - 2.0\rho_0$)

$$Y_e = \frac{n_e}{n_p + n_n} \approx \frac{n_e}{n_n} \approx 0.005647 \left(\frac{\rho}{\rho_0} \right), (10)$$

➤ Inserting Eq.(10) into Eq.(9), we get

$$E_F(e) = 60 \times \left(\frac{\rho}{\rho_0} \right)^{2/3} \text{ MeV} \quad (11)$$



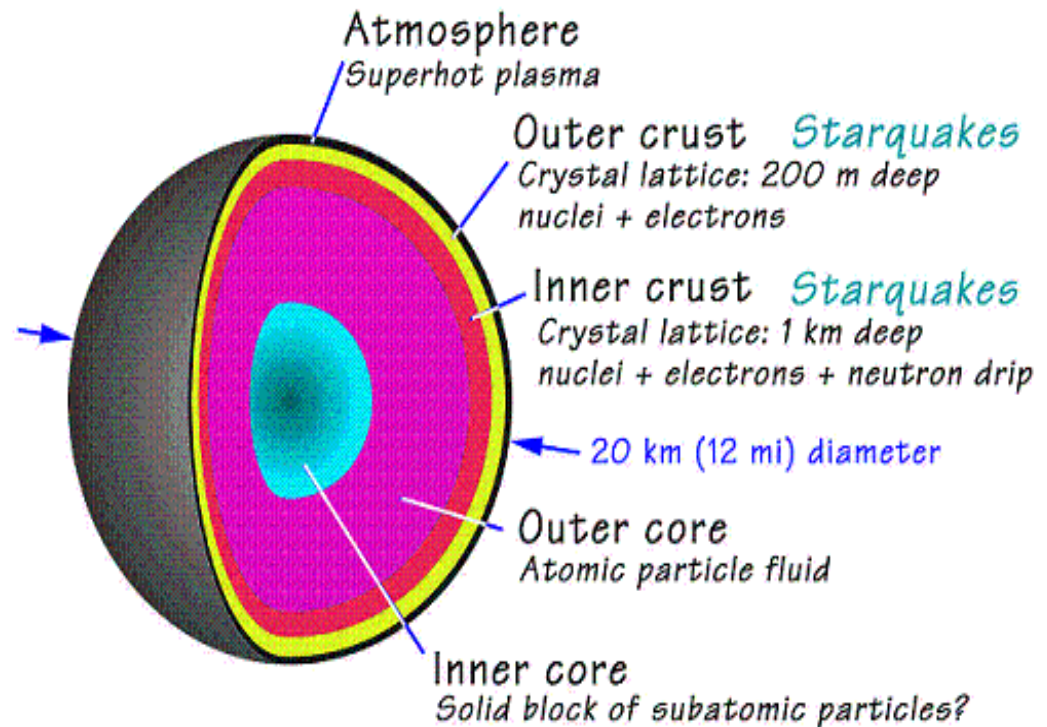
Inserting Eq.(10) into Eq.(11), we get

$$\begin{aligned} E_F(e) &= 60 \times \left(\frac{\rho}{\rho_0} \right)^{\frac{1}{3}} \left(\frac{\rho}{\rho_0} \right)^{\frac{1}{3}} = 60 \times \left(\frac{\rho}{\rho_0} \right)^{\frac{1}{3}} \left(\frac{\frac{\rho_0 Y_e}{0.005647}}{\rho_0} \right)^{\frac{1}{3}} \\ &= 60 \times \left(\frac{\rho}{\rho_0} \right)^{\frac{1}{3}} \left(\frac{Y_e}{0.005647} \right)^{\frac{1}{3}} \text{ (MeV)}. \end{aligned} \quad (12)$$

Application conditions:

$$1. B \ll B^* = 4.4 \times 10^{13} \text{ G} \quad 2. \rho \geq 10^7 \text{ g} \cdot \text{cm}^{-3}$$

Using reliable equations of state (EOSs) and numerical simulations, we will get one-to-one relationship between the electron fraction and matter density at different depths in a NS, then obtain the value of Fermi energy of electrons given any density .





Numerical simulation (I)

- The studies of nucleon matter using Argonne v18 two-nucleon interaction (**Av18**) and Urbana IX three nucleon interaction (**UIX**) indicated that there is a possibility of a transition to a neutral pion condensed phase for both symmetric and pure neutron matter;
- Akmal, Pandharipande, & Ravenhall(1998) (APR98) investigated the properties of dense nucleon matter and the structure of NSs, and provided an excellent fit to all of the nucleon-nucleon scattering data in the Nijmegen data.
- In APR98, the authors not only considered thenon-relativistic calculations with **Av18** and **Av18+UIX** models for nuclear forces, but also described the relativistic boost interaction model (denoted as δv) with and without three-nucleon interaction (**UIX***).
- The difference between these two models lies in that whether the effect of three-nucleon interaction (TNI) is considered. These two models can be regarded as more realistic models.

(Akmal, Pandharipande, & Ravenhall 1998)



According to the APR98, the effective interactions have same form

$$H = [\hbar^2/(2m) + (p_3 + (1 - Y_p)p_5) \rho e^{-p_4\rho}] \tau_n + (\hbar^2/(2m) + (p_3 + Y_p p_5) \rho e^{-p_4\rho}) \tau_p + g(\rho, Y_p = 0.5) (1 - (1 - 2Y_p)^2) + g(\rho, Y_p = 0)(1 - 2Y_p)^2,$$

where $\rho = \rho_n + \rho_p$ at zero temperature, and

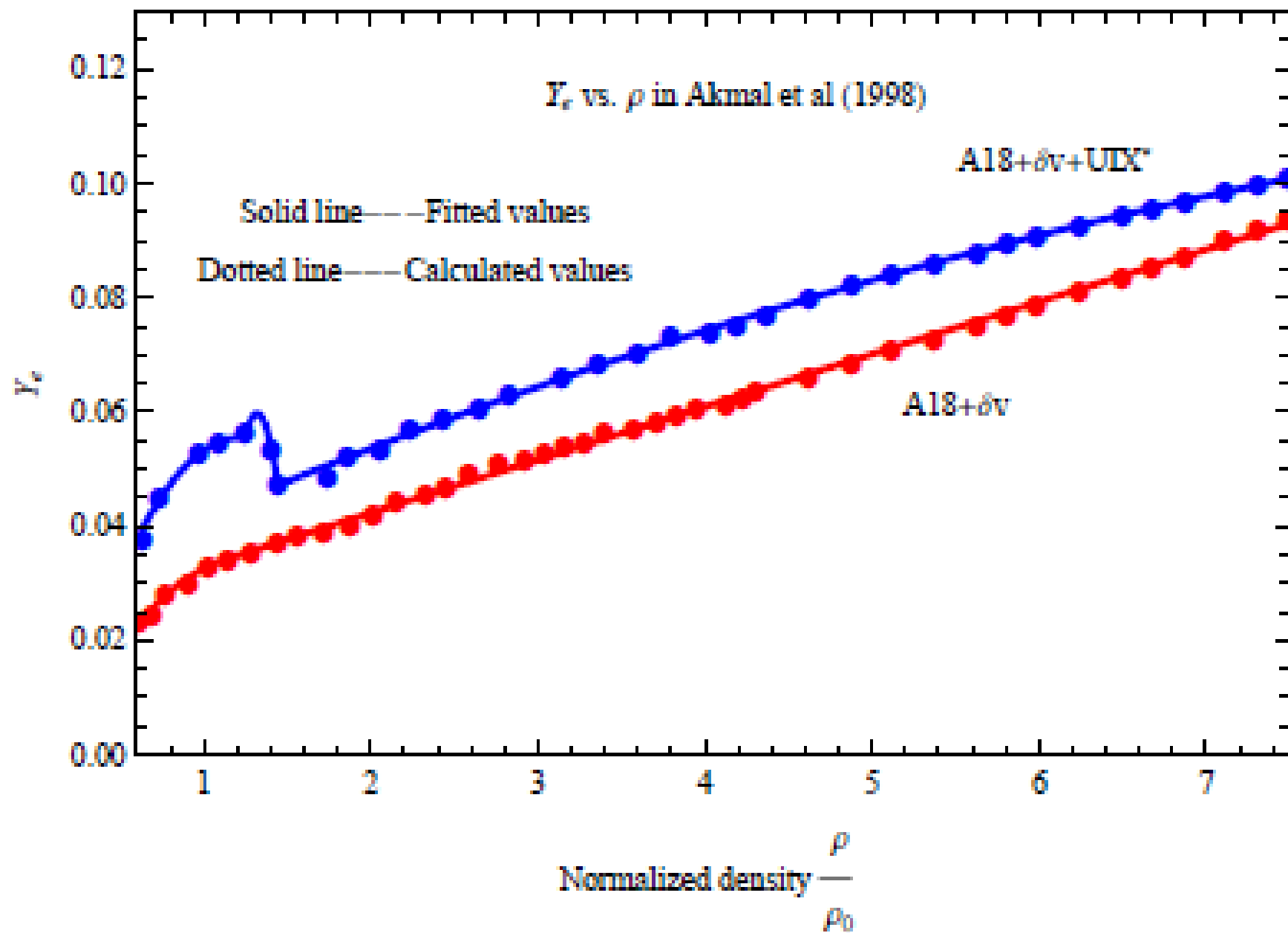
$$\tau_p = \frac{3}{5}(3\pi^2\rho)^{\frac{2}{3}}Y_p^{\frac{5}{3}}, \tau_n = \frac{3}{5}(3\pi^2\rho)^{\frac{2}{3}}(1 - Y_p)^{\frac{5}{3}}.$$

Table 1 Parameter values for $Av18 + \delta v + UIX^*$ and $Av18 + \delta v$ models.

model	p_1	p_2	p_6	p_7	p_8	p_9	p_{10}	p_{11}	p_{12}	p_{13}
$Av18 + \delta v + UIX^*$	337.2	-382.0	-19.1	214.6	-384.0	6.4	69.0	-33.0	0.35	0
$A18 + \delta v$	281.0	-151.1	-10.6	210.1	-158.0	5.88	58.8	-15.0	-0.2	-0.9
model	p_{14}	p_{15}	p_{16}	p_{17}	p_{18}	p_{19}	p_{20}	p_{21}	--	--
$Av18 + \delta v + UIX^*$	0	287.0	-1.54	175.0	-1.45	0.32	0.195	0	--	--

Table 2 Partial values of n_B , ρ , Y_e and $E_F(e)$ for $Av18 + \delta v + UIX^*$ and $Av18 + \delta v$ models.

<i>Av18 + δv</i>									
n_B (fm ⁻³)	Matter-density (g cm ⁻³)	Y_e (%)	$E_F(e)$ (MeV)	$E_F^\dagger(e)$ (MeV)	n_B (fm ⁻³)	Matter-density (g cm ⁻³)	Y_e (%)	$E_F(e)$ (MeV)	$E_F^\dagger(e)$ (MeV)
0.10	1.661×10^{14}	2.395	81.60	81.32	0.67	1.113×10^{15}	6.237	211.64	211.96
0.17	2.178×10^{14}	2.789	102.45	102.19	0.74	1.229×10^{15}	6.620	223.15	223.33
0.23	3.819×10^{14}	3.683	124.33	124.03	0.82	1.362×10^{15}	7.068	236.02	236.32
0.30	4.982×10^{14}	4.165	141.52	141.02	0.90	1.495×10^{15}	7.528	248.63	248.76
0.37	6.144×10^{14}	4.590	156.76	156.76	0.96	1.594×10^{15}	7.881	257.95	258.21
0.41	6.808×10^{14}	4.820	164.88	164.56	1.00	1.661×10^{15}	8.121	264.11	264.43
0.45	7.473×10^{14}	5.043	172.67	172.36	1.04	1.727×10^{15}	8.365	270.23	270.65
0.49	8.137×10^{14}	5.262	180.17	180.10	1.07	1.777×10^{15}	8.552	274.23	274.54
0.57	9.465×10^{14}	5.695	194.55	194.67	1.14	1.893×10^{15}	8.991	285.42	285.56
0.64	1.063×10^{15}	6.073	206.59	206.65	1.20	1.993×10^{15}	9.378	294.45	294.64
<i>A18 + $\delta v + UIX^*$</i>									
0.10	1.661×10^{14}	3.707	94.38	94.09	0.67	1.113×10^{15}	7.633	226.38	226.65
0.17	2.178×10^{14}	4.701	121.94	121.38	0.74	1.229×10^{15}	8.001	237.71	237.93
0.23	3.819×10^{14}	4.791	135.72	135.25	0.82	1.362×10^{15}	8.404	250.04	250.21
0.30	4.982×10^{14}	5.274	153.11	152.81	0.90	1.495×10^{15}	8.789	261.99	262.23
0.37	6.144×10^{14}	5.796	169.44	169.17	0.96	1.594×10^{15}	9.068	270.29	270.65
0.41	6.808×10^{14}	6.073	178.09	177.88	1.00	1.661×10^{15}	9.251	275.84	275.99
0.45	7.473×10^{14}	6.385	186.33	186.01	1.04	1.727×10^{15}	9.429	280.26	280.54
0.49	8.137×10^{14}	6.592	194.23	194.03	1.07	1.777×10^{15}	9.563	285.26	285.76
0.57	9.465×10^{14}	7.073	209.12	209.37	1.14	1.893×10^{15}	9.864	294.37	294.57
0.64	1.063×10^{15}	7.468	221.54	221.33	1.20	1.993×10^{15}	10.12	301.98	302.46





By performing 2nd order polynomial fitting, we obtain

$$Y_e = -0.01232 + 0.1184 \varrho - 0.0572 \varrho^2,$$

$$Y_e = -1.4321 + 2.3246 \varrho - 0.9085 \varrho^2,$$

$$Y_e = 0.0291 + 0.0146 \varrho - 5.68 \times 10^{-4} \varrho^2,$$

for $\varrho \sim 0.593 - 1.190$ ($\rho \sim (1.661 \times 10^{14} - 3.331 \times 10^{14}) \text{ g cm}^{-3}$), $\varrho \sim 1.190 - 1.366$ ($\rho \sim (3.331 \times 10^{14} - 3.826 \times 10^{14}) \text{ g cm}^{-3}$), and $\varrho \sim 1.366 - 7.118$ ($\rho \sim (3.826 \times 10^{14} - 1.993 \times 10^{15}) \text{ g cm}^{-3}$), respectively, where $n_{max} = 2$ is assumed. When at the density-node of $\varrho = 1.190$, the “jump” of the electron fraction is 0.0007, corresponding to a relative variation $|\Delta Y_e / Y_e| \sim 1.4\%$, while at the point $\varrho = 1.366$, the “jump” is about 0.0006, corresponding to a relative variation of 1.2%.



As to the $Av18+\delta v$ model, the data of Y_e are divided into two groups according to their change trend. In the same way, we obtain

$$Y_e = -0.0105 + 0.07487 \varrho - 0.03053 \varrho^2,$$

$$Y_e = 0.0236 + 0.00991 \varrho - 2.317 \times 10^{-5} \varrho^2$$

for $\varrho \sim 0.593 - 0.984$ ($\rho \sim (1.661 \times 10^{14} - 2.755 \times 10^{14}) \text{ g cm}^{-3}$), and $\varrho \sim 0.984 - 7.118$ ($\rho \sim (2.755 \times 10^{14} - 1.993 \times 10^{15}) \text{ g cm}^{-3}$), respectively. When at density-node of $\varrho = 0.984$, the change $|\Delta Y_e| = 0.0006$, corresponding to a relative variation of 2.1%, which ensures the continuity of two analytical expressions. The differences of Y_e between the data and the fits are typically $\sim 10^{-3}$ or better, the relative differences are smaller than 1%, and the maximum error is about 0.004 also at the low density end.



Relativistic mean field (RMF)

- The relativistic-mean-field (RMF) theory, which has become standard method to study nuclear matter and finite-nuclei properties.
- According to RMF models, the strong interaction between baryons is mediated by the exchange of isoscalar scalar and vector mesons σ , ω , isovector vector meson ρ .
- There are two additional strange mesons namely isoscalar scalar σ^* and vector ϕ mesons considered by some authors (e.g., Schaffner & Mishustin 1996; Xu et al. 2012).

We adopt the five-mesons-model in RMF, the lagrangian has the



The lagrangian of five-mesons-model

$$\begin{aligned} L = & \sum_B \bar{\psi}_B [i\gamma_\mu \partial^\mu - (m_B - g_{\sigma B} \sigma - g_{\sigma^* B} \sigma^*) \\ & - g_{\rho B} \gamma_\mu \tau \cdot \rho^\mu - g_{\omega B} \gamma_\mu \omega^\mu - g_{\phi B} \gamma_\mu \phi^\mu] \psi_B \\ & + \frac{1}{2} (\partial_\mu \sigma \partial^\mu \sigma - m_\sigma^2 \sigma^2) + \frac{1}{2} (\partial_\nu \sigma^* \partial^\nu \sigma^* \\ & - m_{\sigma^*}^2 \sigma^{*2}) - \frac{1}{4} W^{\mu\nu} W_{\mu\nu} - \frac{1}{4} R^{\mu\nu} R_{\mu\nu} \\ & + \frac{1}{2} m_\rho^2 \rho_\mu \rho^\mu - \frac{1}{4} P^{\mu\nu} P_{\mu\nu} + \frac{1}{2} m_\omega^2 \omega_\mu \omega^\mu \\ & - \frac{1}{3} a \sigma^3 - \frac{1}{4} b \sigma^4 + \frac{1}{2} m_\phi^2 \phi_\mu \phi^\mu \end{aligned}$$

where $W_{\mu\nu} = \partial_\mu \omega_\nu - \partial_\nu \omega_\mu$, $R_{\mu\nu} = \partial_\mu \rho_\nu - \partial_\nu \rho_\mu$ and $P_{\mu\nu} = \partial_\mu \phi_\nu - \partial_\nu \phi_\mu$ denote the field tensors of ω , ρ and ϕ mesons, respectively.



The meson field equations in NSs are as follows

$$\sum_B g_{\sigma B} \rho_{SB} = m_{\sigma}^2 \sigma + a \sigma^2 + b \sigma^3,$$

$$\sum_B g_{\omega B} \rho_B = m_{\omega}^2 \omega_0 + c_3 \omega_0^3,$$

$$\sum_B g_{\rho B} \rho_B I_{3B} = m_{\rho}^2 \rho_0,$$

$$\sum_B g_{\sigma^* B} \rho_{SB} = m_{\sigma^*}^2 \sigma^*,$$

$$\sum_B g_{\phi B} \rho_B = m_{\phi}^2 \phi_0,$$



At $T=0$ the lepton chemical potentials are expressed by

$$\mu_l = \sqrt{k_F^l{}^2 + m_l^2}, \quad (\text{fm}^{-1})$$

The charge neutrality condition is given by

$$\sum_B q_B \rho_B - n_e - n_\mu = 0,$$



By solving the coupled equations self-consistently at a given density, we get the total energy state density and total pressure

$$\begin{aligned}\varepsilon &= \sum_B \frac{1}{\pi^2} \int_0^{k_F^B} \sqrt{k^2 + m_B^{*2}} k^2 dk + \frac{1}{2} m_\sigma^2 \sigma^2 + \frac{1}{3} g_2 \sigma^3 + \frac{1}{4} g_3 \sigma^4 \\ &\quad + \frac{1}{2} m_\omega^2 \omega^2 + \frac{3}{4} c_3 \omega^4 + \frac{1}{2} m_\rho^2 \rho^2 + \sum_l \frac{1}{\pi^2} \int_0^{k_F^l} \sqrt{k^2 + m_l^2} k^2 dk, \\ P &= \frac{1}{3} \sum_B \frac{1}{\pi^2} \int_0^{k_F^B} \frac{k^4 dk}{\sqrt{k^2 + m_B^{*2}}} - \frac{1}{2} m_\sigma^2 \sigma^2 - \frac{1}{3} g_2 \sigma^3 - \frac{1}{4} g_3 \sigma^4 \\ &\quad + \frac{1}{2} m_\omega^2 \omega^2 + \frac{1}{4} c_3 \omega^4 + \frac{1}{2} m_\rho^2 \rho^2 + \frac{1}{3} \sum_l \frac{1}{\pi^2} \int_0^{k_F^l} \frac{k^4 dk}{\sqrt{k^2 + m_l^2}}.\end{aligned}$$

Table 7 Saturation properties, meson-nucleon couplings and self-coupling constants of three RMF models.

Model	ρ_0 fm^{-3}	E_0 MeV	K_0 MeV	m^*	K' MeV	J MeV	L_0 MeV	K_{sym}^0 MeV	Q_{sym}^0 MeV	$K_{\tau,V}^0$ MeV
NL3	0.148	-16.24	271.53	0.60	-202.91	37.40	118.53	100.88	181.31	-698.85
TMA	0.147	-16.02	318.15	0.635	572.12	30.66	90.14	10.75	-108.74	-367.99
GM1(SU3)	0.153	-16.33	300.50	0.70	215.66	32.52	94.02	17.98	25.01	-478.64
Model	m_N MeV	m_σ MeV	m_ω MeV	m_ρ MeV	$g_{\sigma N}$ fm^{-1}	$g_{\omega N}$ fm^{-1}	$g_{\rho N}$ fm^{-1}	a fm^{-1}	b fm^{-1}	c_3 fm^{-1}
NL3	939.0	508.194	782.50	763.0	10.217	12.868	4.474	-10.431	-28.885	0
TMA	939.0	519.151	781.95	768.1	10.055	12.842	3.800	-0.328	38.862	151.590
GM1(SU3) [†]	938.0	550	783.0	770.0	4.10	10.26	4.10	12.28	-8.98	0

Note: [†]. For the GM1(SU3) parameter set, the meson masses $m_{\sigma^*} = 975.0$ MeV, and $m_{\phi^*} = 1020.0$ MeV, the meson- hyperon couplings $g_{\sigma\Lambda} = 6.170 \text{ fm}^{-1}$, $g_{\sigma\Sigma} = 1020.0 \text{ fm}^{-1}$, $g_{\sigma^*\Lambda} = 5.412 \text{ fm}^{-1}$, and $g_{\sigma^*\Lambda} = 11.516 \text{ fm}^{-1}$.

Table 8 Partial calculations of n_B , n_e , Y_e and $E_F(e)$ for TMA parameter set.

n_B (fm ⁻³)	n_e (cm ⁻³)	Y_e	$E_F(e)$ (MeV)	ε (fm ⁻⁴)	P (fm ⁻⁴)
3.808×10 ⁻⁶	0	0	0.04921	1.779×10 ⁻⁵	3.41×10 ⁻¹⁰
1.312×10 ⁻⁵	0	0	0.11482	6.202×10 ⁻⁵	2.64×10 ⁻⁹
0.00106	6.202×10 ³¹	0.0000583	2.4698	0.0050	2.708×10 ⁻⁶
0.0434	3.3639×10 ³⁵	0.00775	42.459	0.2073	2.097×10 ⁻⁴
0.1106	3.5155×10 ³⁶	0.03179	92.825	0.53086	0.00767
0.1442	6.6243×10 ³⁶	0.04594	114.65	0.69582	0.01835
0.1666	9.0084×10 ³⁶	0.05407	127.02	0.80746	0.02822
0.2786	2.3829×10 ³⁷	0.08553	175.67	1.3899	0.11426
0.3066	2.8026×10 ³⁷	0.09141	185.43	1.5425	0.14544
0.3696	3.7847×10 ³⁷	0.1024	204.96	1.8971	0.22919
0.4326	4.7996×10 ³⁷	0.11095	221.85	2.2675	0.33046
0.5852	7.327×10 ³⁷	0.12521	255.45	3.2303	0.63688
0.6286	8.0579×10 ³⁷	0.12819	263.67	3.5207	0.73716
0.6846	9.0078×10 ³⁷	0.13158	273.65	3.9058	0.87369
0.7826	1.0689×10 ³⁸	0.13658	289.71	4.6073	1.1297
0.8764	1.2319×10 ³⁸	0.14057	303.75	5.3099	1.3921
0.9436	1.3501×10 ³⁸	0.14308	313.17	5.8311	1.5892
1.0528	1.5444×10 ³⁸	0.14669	327.52	6.7083	1.9239
1.1704	1.7567×10 ³⁸	0.15009	341.89	7.6928	2.3017
1.2110	1.8307×10 ³⁸	0.15117	346.63	8.0418	2.4360
1.2278	1.8614×10 ³⁸	0.15161	348.56	8.1875	2.4921
1.2614	1.9231×10 ³⁸	0.15246	352.37	8.4813	2.6053
1.2950	1.9850×10 ³⁸	0.15328	356.11	8.7781	2.7196
1.3202	2.0315×10 ³⁸	0.15388	358.87	9.0027	2.8062
1.3370	2.0627×10 ³⁸	0.15427	360.69	9.1533	2.8642
1.3538	2.0938×10 ³⁸	0.15466	362.50	9.3047	2.9225
1.400	2.1798×10 ³⁸	0.15570	367.40	9.7247	3.0844

Table 9 Partial calculations of n_B , n_e , Y_e and $E_F(e)$ for GM1(SU3) parameter set.

n_B (fm ⁻³)	n_e (cm ⁻³)	Y_e	$E_F(e)$ (MeV)	n_B (fm ⁻³)	n_e (cm ⁻³)	Y_e	$E_F(e)$ (MeV)
0.00153	1.526×10^{33}	0.0000997	3.30	0.42993	4.962×10^{38}	0.1154	224.32
0.0153	3.026×10^{35}	0.00198	19.03	0.49725	6.145×10^{38}	0.1236	240.90
0.02601	1.079×10^{36}	0.00415	29.07	0.56763	7.395×10^{38}	0.1303	256.23
0.03519	2.248×10^{36}	0.00639	37.12	0.60894	8.132×10^{38}	0.1335	264.48
0.0459	4.306×10^{36}	0.00938	46.10	0.65943	9.037×10^{38}	0.1370	273.94
0.05967	8.201×10^{36}	0.01374	57.14	0.70074	9.779×10^{38}	0.1396	281.25
0.07191	1.297×10^{37}	0.01804	66.58	0.78029	1.122×10^{39}	0.1438	294.42
0.09486	2.553×10^{37}	0.02691	83.44	0.85986	1.267×10^{39}	0.1473	306.60
0.10404	3.194×10^{37}	0.0307	89.91	0.86139	1.270×10^{39}	0.1474	306.82
0.11016	3.667×10^{37}	0.0333	94.14	0.88281	1.309×10^{39}	0.1483	309.95
0.13005	5.450×10^{37}	0.0419	107.43	0.91035	1.360×10^{39}	0.1493	313.90
0.14076	6.492×10^{37}	0.04612	113.88	0.95778	1.447×10^{39}	0.1511	320.50
0.17289	9.952×10^{37}	0.05756	131.31	1.0557	1.629×10^{39}	0.1543	333.42
0.18513	1.140×10^{38}	0.0616	137.41	1.1047	1.721×10^{39}	0.1558	339.57
0.22491	1.657×10^{38}	0.07366	155.62	1.2378	1.973×10^{39}	0.1594	355.41
0.2754	2.393×10^{38}	0.08688	175.91	1.3235	2.138×10^{39}	0.1615	365.01
0.34272	3.471×10^{38}	0.10129	199.14	1.3908	2.268×10^{39}	0.1631	372.26
0.39933	4.431×10^{38}	0.11097	216.02	1.530	2.539×10^{39}	0.1660	386.56

Table 11 Partial calculations of n_B , n_e , Y_e and $E_F(e)$ for NL3 parameter set.

n_B (fm ⁻³)	n_e (cm ⁻³)	Y_e	$E_F(e)$ (MeV)	ε (fm ⁻⁴)	P (fm ⁻⁴)
1.48×10^{-8}	0	0	0.001	7.55×10^{-8}	3.606×10^{-14}
1.036×10^{-7}	0	0	0.0039	4.23×10^{-7}	6.984×10^{-13}
7.400×10^{-5}	0	0	0.38889	0.000352	4.204×10^{-8}
3.108×10^{-4}	3.7149×10^{30}	1.2×10^{-5}	1.0747	0.0014	3.901×10^{-7}
0.00132	1.2348×10^{32}	9.4×10^{-5}	3.0825	0.00627	3.125×10^{-6}
0.00592	3.9553×10^{33}	6.7×10^{-4}	9.6678	0.02822	1.841×10^{-5}
0.04292	4.8659×10^{35}	0.01134	48.018	0.2050	5.987×10^{-4}
0.07104	1.7196×10^{36}	0.0242	73.138	0.34024	0.00285
0.10064	4.0873×10^{36}	0.04061	97.607	0.48403	0.00795
0.14208	8.9505×10^{36}	0.06300	126.75	0.68868	0.02053
0.17168	1.3163×10^{37}	0.07667	144.14	0.83771	0.03452
0.20276	1.8191×10^{37}	0.08972	160.55	0.99734	0.05631
0.23088	2.3149×10^{37}	0.10026	173.98	1.1453	0.08543
0.29156	3.4434×10^{37}	0.1181	198.61	1.4804	0.19431
0.32116	3.9935×10^{37}	0.12435	208.66	1.6542	0.27455
0.35224	4.5623×10^{37}	0.12952	218.13	1.8455	0.37757
0.41144	5.625×10^{37}	0.13672	233.9	2.2377	0.62107
0.44252	6.1771×10^{37}	0.13959	241.32	2.4591	0.77093
0.47212	6.7017×10^{37}	0.14195	247.96	2.6802	0.92646
0.50172	7.2266×10^{37}	0.14404	254.28	2.9114	1.0939

0.59052	8.8109×10^{37}	0.14921	271.64	3.6665	1.6631
0.61124	9.1836×10^{37}	0.15025	275.42	3.8560	1.8098
0.64084	9.7183×10^{37}	0.15165	280.67	4.1356	2.0283
0.67488	1.0337×10^{38}	0.15316	286.50	4.4698	2.2923
0.70152	1.0823×10^{38}	0.15429	290.93	4.7409	2.5083
0.73112	1.1367×10^{38}	0.15547	295.72	5.0519	2.7579
0.76072	1.1913×10^{38}	0.15661	300.38	5.3733	3.0176
0.79328	1.2518×10^{38}	0.1578	305.38	5.738	3.3148
0.82288	1.307×10^{38}	0.15884	309.81	6.0816	3.5954
0.86136	1.3793×10^{38}	0.16013	315.41	6.5428	3.9749
0.89392	1.4407×10^{38}	0.16117	320.03	6.9466	4.309
0.92056	1.4913×10^{38}	0.162	323.73	7.2862	4.5912
0.95016	1.5477×10^{38}	0.16289	327.76	7.6732	4.914
0.98124	1.6072×10^{38}	0.1638	331.91	8.0905	5.2634
1.0034	1.6498×10^{38}	0.16442	334.82	8.3955	5.5196
1.0227	1.6869×10^{38}	0.16495	337.31	8.6645	5.746
1.0523	1.7442×10^{38}	0.16575	341.08	9.0867	6.1023
1.0922	1.8218×10^{38}	0.1668	346.07	9.6727	6.5987
1.1233	1.8825×10^{38}	0.16758	349.87	10.141	6.9969
1.1514	1.9376×10^{38}	0.16827	353.25	10.575	7.3664
1.2151	2.0629×10^{38}	0.16978	360.71	11.590	8.2346
1.2713	2.1745×10^{38}	0.17104	367.10	12.526	9.0387
1.2965	2.2246×10^{38}	0.17159	369.90	12.956	9.4097
1.3424	2.3164×10^{38}	0.17256	374.91	13.760	10.104
1.3705	2.3728×10^{38}	0.17314	377.93	14.264	10.541
1.4119	2.4563×10^{38}	0.17397	382.31	15.024	11.200
1.4431	2.5191×10^{38}	0.17457	385.54	15.607	11.707
1.4800	2.5941×10^{38}	0.17527	389.33	16.315	12.325

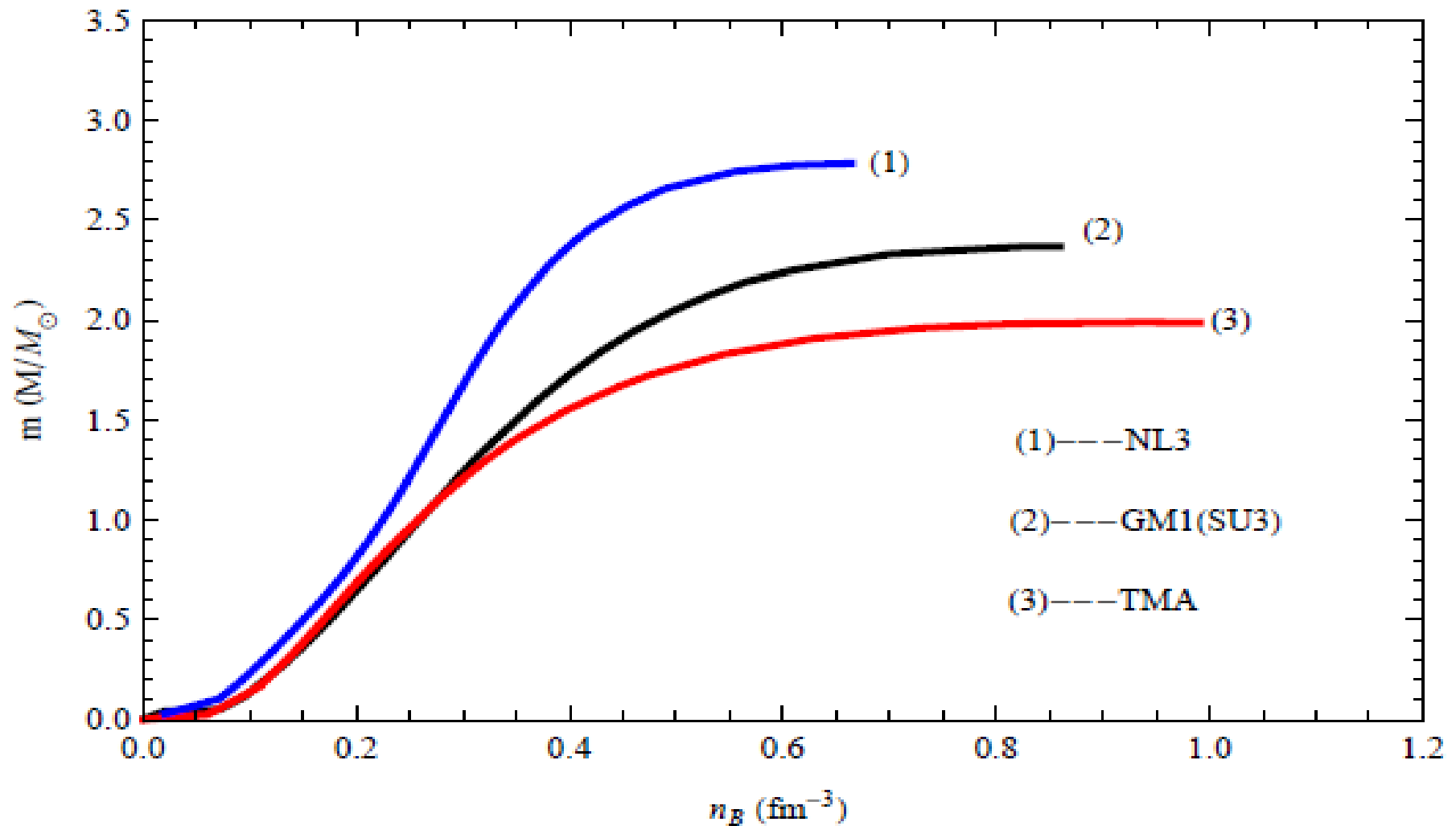
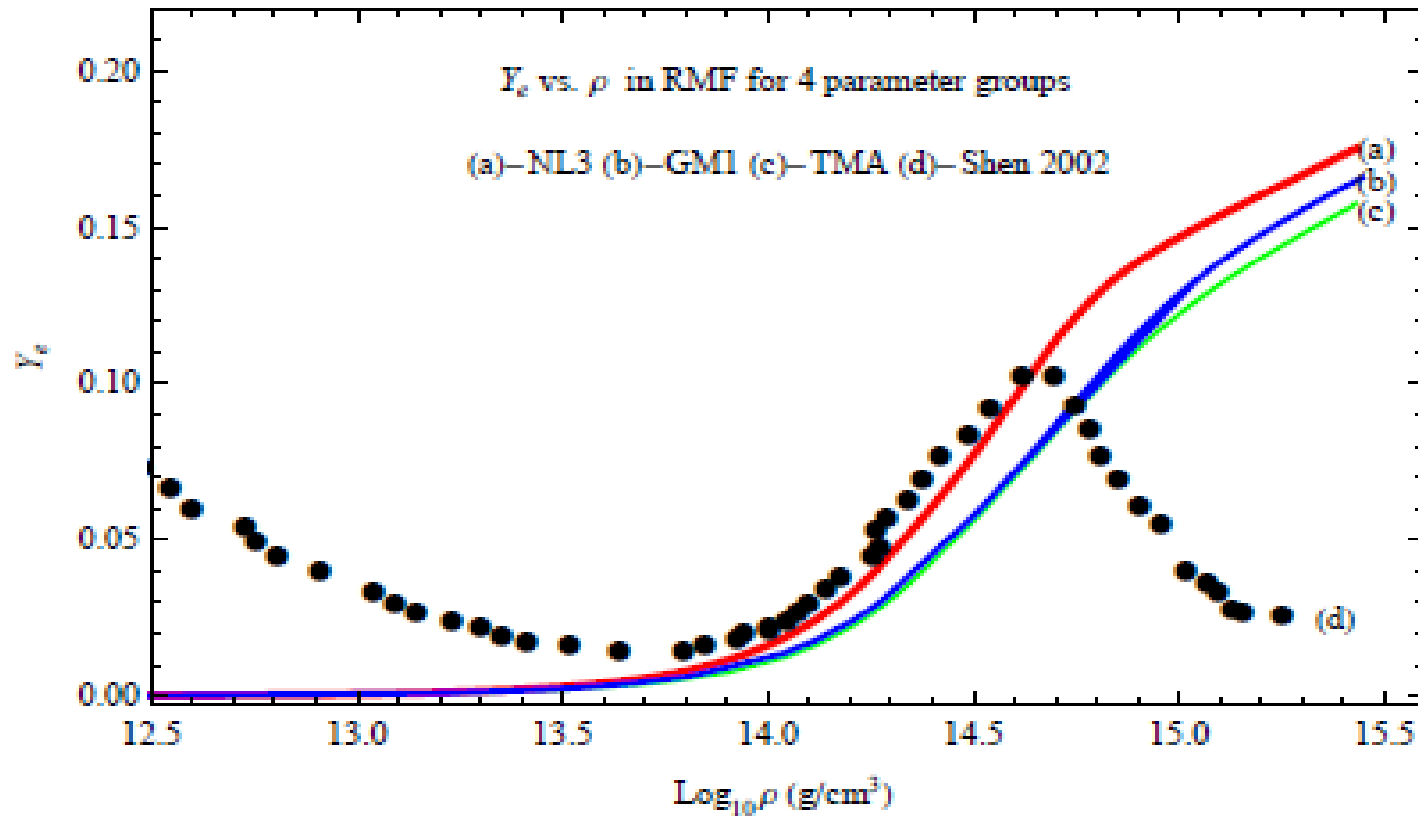


Fig. 16 The relations of m_{max} and $n_B(c)$ for RMF models.



The relation of Y_e and ρ in four MMF models



Analytical expressions(1)

We obtain a set of analytical expressions of Y_e for TMA parameter set

$$Y_e = -0.00316 + 0.05258 \rho - 0.00514 \rho^2,$$
$$Y_e = 0.08235 + 0.0124 \rho - 5.04 \times 10^{-4} \rho^2,$$

for $\rho \sim (6.918 \times 10^{11} - 9.380 \times 10^{14})$ and $(9.380 \times 10^{14} - 2.690 \times 10^{15}) \text{ g cm}^{-3}$, respectively. At the midpoint of $2.988 \times 10^{14} \text{ g cm}^{-3}$, the "jump" of Y_e is about 2.8×10^{-3} , and its relative variation $\sim 2.5\%$ confirming the continuities of two expressions above. The typical differences between the fit and the data are $10^{-3} - 10^{-4}$, and their relative differences are typically $10^{-2} - 10^{-3}$. The maximum absolute deviation and relative error are 4.5×10^{-3} and 3% , respectively, at the high-density end, due to uncertainty of the EoS.



Analytical expressions

We obtain a set of analytical expressions of Y_e for GM1(SU3) parameter set

$$Y_e = -0.00298 + 0.0526 \varrho - 0.00494 \varrho^2,$$

$$Y_e = 0.07663 + 0.0138 \varrho - 5.99 \times 10^{-4} \varrho^2,$$

for $\rho \sim (6.917 \times 10^{11} - 8.036 \times 10^{14})$ and $(8.036 \times 10^{14} - 2.690 \times 10^{15}) \text{ g cm}^{-3}$, respectively. At the midpoint of $8.036 \times 10^{14} \text{ g cm}^{-3}$, the "jump" of Y_e is about 4×10^{-3} , and its relative variation $\sim 3.7\%$, which also ensures the continuities of two expressions above. The typical differences between the fit and the data are $10^{-3} - 10^{-4}$, and their relative differences are typically 10^{-3} . The maximum absolute deviation and relative error are 3.2×10^{-3} and 3% , respectively, at the high-density end.

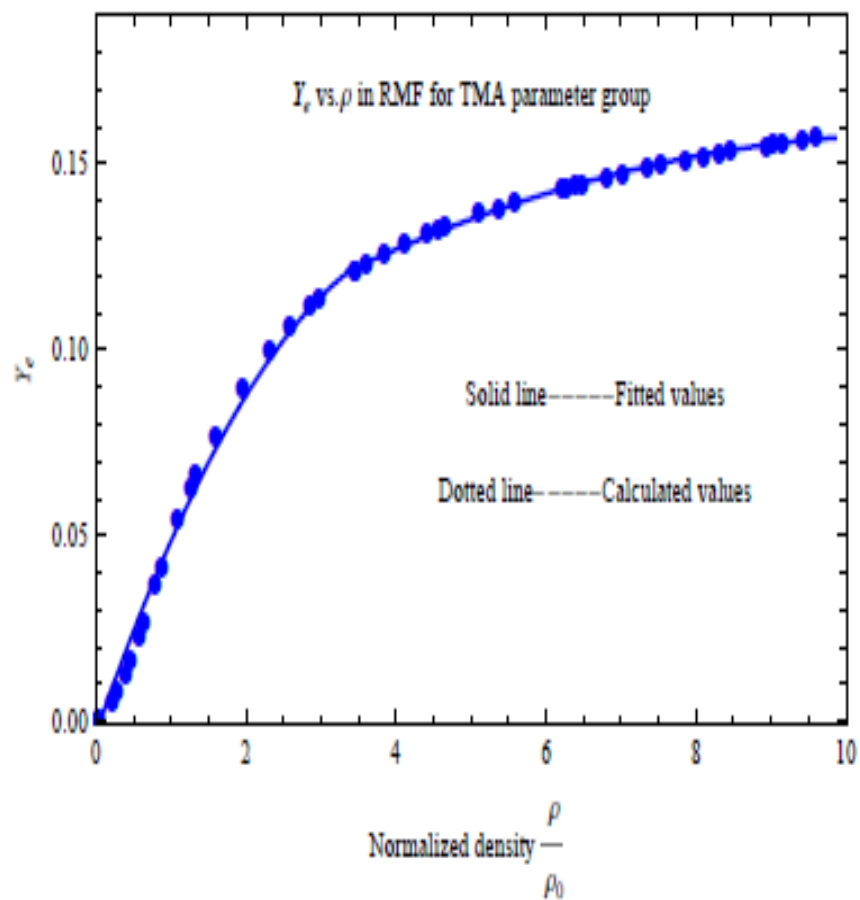


Analytical expressions (3)

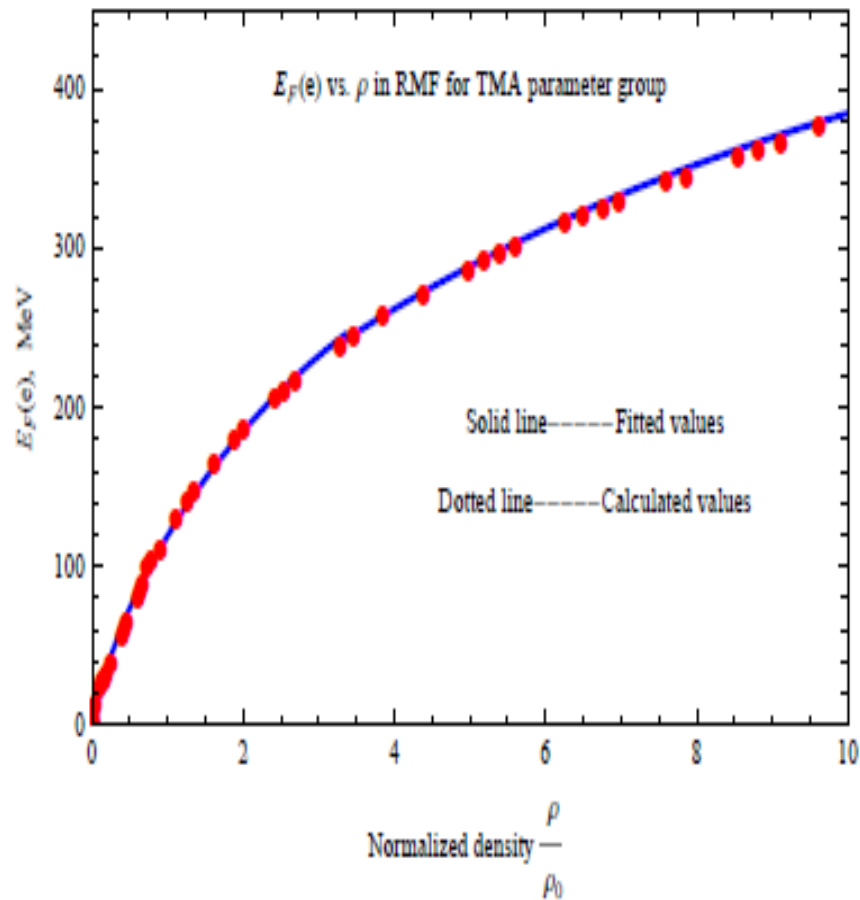
We obtain a set of analytical expressions of Y_e for NL3 parameter set

$$Y_e = -0.00436 + 0.0749 \varrho - 0.00851 \varrho^2,$$
$$Y_e = 0.11556 + 0.00931 \varrho - 3.52 \times 10^{-4} \varrho^2,$$

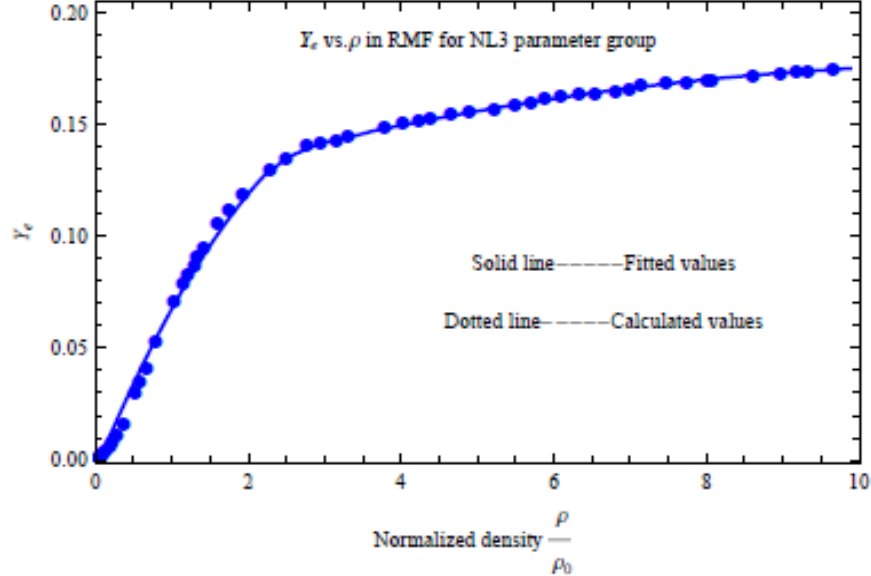
for $\rho \sim (5.688 \times 10^{11} - 7.420 \times 10^{14})$ and $(7.420 \times 10^{14} - 2.708 \times 10^{15})$ g cm⁻³, respectively. At the midpoint of 7.420×10^{14} g cm⁻³, the "jump" of Y_e is about 3.4×10^{-3} , and its relative variation $\sim 2.5\%$, which also ensures the continuities of two expressions above. The typical differences between the fit and the data and their relative differences are similar to those of T-MA parameter set. The maximum absolute deviation and relative error are 3.5×10^{-3} and 2%, respectively, at the high-density end.



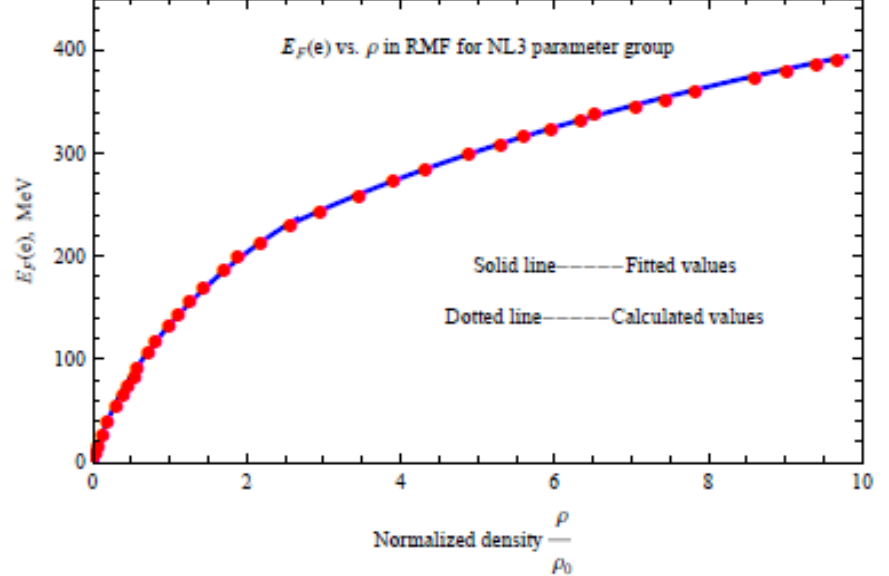
(a)



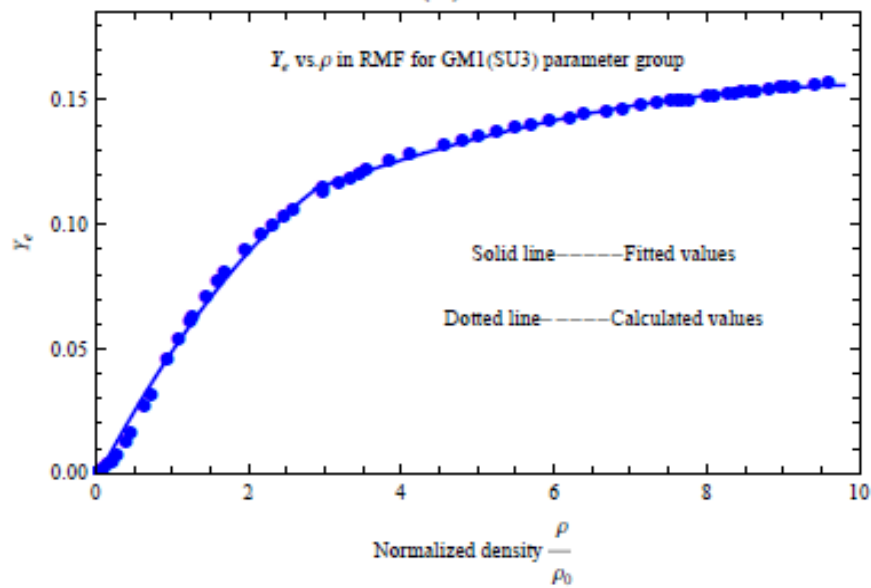
(b)



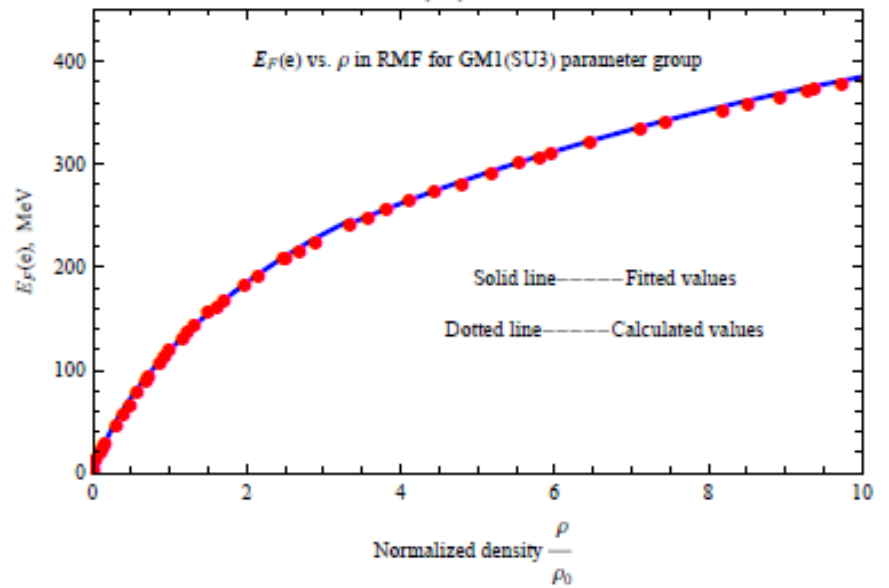
(c)



(d)



(e)



(f)



Conclusions

- We deduce a uniform formula of Fermi energy degenerate and relativistic electrons in the weak-magnetic field approximation.
- We performed numerical simulations firstly in APR98, then in RM models, and obtained a number of analytical representations of Y_e .
- Since Y_e and $EF(e)$ are important in assessing cooling rate of a NS and the possibility of kaon/pion condensation in the NS interior, the analytical representations obtained will be very useful in the future study on thermal evolution of a NS and the EoS of NS's matter under extreme conditions, though our methods are indeed simple.



中国科学院新疆天文台
XINJIANG ASTRONOMICAL OBSERVATORY, CAS

*Thank you for
your attention!*